Two phase residence time distribution in a modified twin screw extruder

L. Prat [a], P. Guiraud [a,*], L. Rigal [b], C. Gourdon [a]

[a] *Laboratoire de Génie Chimique, UMR 5503 CNRS/INPT-ENSIGC/UPS, 18 Chemin de la Loge, 31078, Toulouse Cedex 4, France*
[b] *Laboratoire de Chimie Agroindustrielle, UA INRA 31A1010, INP, ENSCT, 118 route de Narbonne-31077, Toulouse Cedex, France*

Abstract

Biomass fractionation is performed with a modified Clextral twin-screw extruder used as a thermo-mechano-chemical reactor. This new process is firstly analyzed. Visual observations, residence time distributions, and global mass balances are used to obtain information about the process phenomena and their coupling. Residence time distributions (RTD) classical models are adopted to represent the experimental plots. The influence of continuous and discrete process parameters upon the RTD of the solid and liquid phases is analyzed.

Keywords: Twin-screw extruder; Biomass fractionation; Polyphasic-flow; Residence time distribution

1. Introduction

An important application domain of twin-screw extruders (TSE) is found in the agro-industry for starch conversion and protein texturization [1,2]. These contactors allow the simultaneous combination of two unit operations: extrusion and cooking, thus performing both physical and chemical transformations of biopolymers in a single step. TSE can also be used as an extractor, to process essential oils [3], lipids [4], or wood pulping [5,6]. It's ability to carry out extraction and chemical reaction in a single continuous reactor makes TSE very valuable for the valorization of agroresource wastes [7]. TSE process economic evaluation are then under investigation [8].

In this work, the application under consideration is the extraction of hemicelluloses from hardwood populus via alkaline solubilization. As a test case, it shall help us to enhance the knowledge of such solid/liquid contactor. The twin-screw extruder is used as a thermo-mechano-chemical reactor for biomass fractionation. N'Diaye et al. (1996) [8,9] have demonstrated the feasibility of the studied process for various vegetable matters. Fig. 1 shows the process operating principle. The machine consists of a seven eight-shaped elements barrel enclosing two corotating intermeshing screws. Solid (wood) and liquid (alkaline solution) are fed into the barrel by the first transport screws and are mixed together in the transport and kneading elements. As the liquid is absorbed by the wood, reaction occurs. Further down, reversed transport screw elements (RSE) cause severe compression of the vegetable matter and allow the separation of the two phases. Liquid phase is then retrieved through a barrel filter located just upstream from the RSE.

In order to promote the TSE in the domain of agroresource valorization, the main goal is to understand its working conditions and the influence of both continuous operating parameters such as the solid and liquid feed rates, the screw speed, the temperature, NaOH percentage in the liquid, and discrete operating parameters such as the screw profile. Modeling and optimization of the functioning of such a reacting contactor, will lead to use a mass transport model in combination of a reactive extraction model. It will then allow to obtain extraction yields. Such an approach has been successfully applied to other polyphasic contactors like extraction columns for instance.

* Corresponding author. Tel.: +33-5-62252375; Fax: +33-5-62252318; e-mail: Pascal.Guiraud@ensigct.fr.

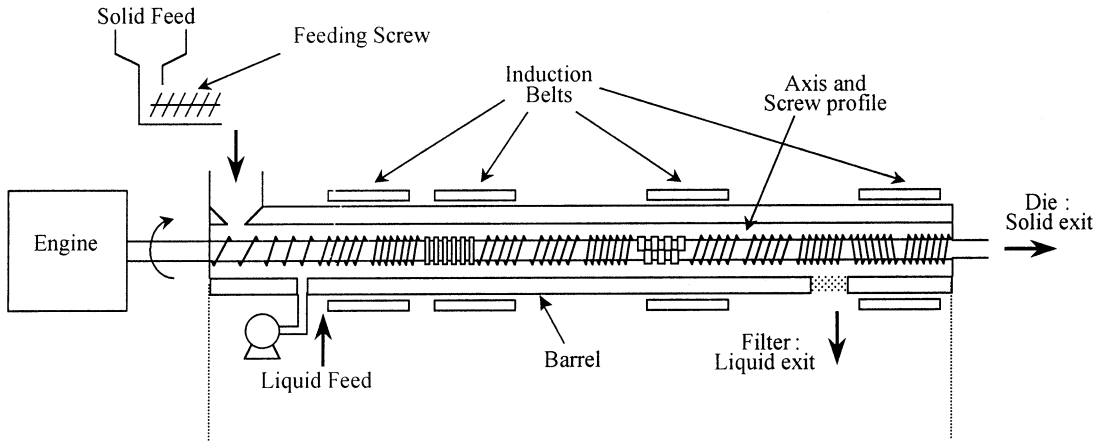

Type	T2F	C2F	C2F	C2F	Mal2	C2F	C2F	C2F	Mal0	C2F	C2F	C2F	C2FC	C2F
Pitch (mm)	66	50	33	25		33	33	25		33	33	25		25
Length (mm)	100	100	100	100	100	100	100	100	100	100	100	100	100	100
Induction			Yes		Yes				Yes				Yes	

T2F

Fig. 1. Global process in a modified CLEXTRAL BC45 TSE.

2. Scope and presentation of the problem

However, the current problem, in a certain way, is quite different from the one relevant to other applications of extrusion. If TSE hydrodynamics for food or polymer begins to be well known [10–12], the two phase flow constituted by vegetable matter/liquid does not allow to adopt the mechanical approach used for other systems for now.

Complexity of the phenomena in this process first lies in the complexity of the vegetable matter itself and second in the important coupling between chemical, mechanical and physical phenomena involved.

Intrinsic physico-chemical properties classically used in chemical engineering are not easily accessible or are difficult to define for the vegetable matter. Moreover, local mass balances are complex and require drastic simplified hypothesis to be solved. Physical properties of the vegetable matter, like compressibility, are subject to thorough changes. Its internal structure is affected by the progress of the reactive extraction as NaOH breaks it, and by internal moisture occurrence. Chemically spreading, the vegetable matter is also uneasy to define. In fact, only general classes of compounds (cellulose, hemicelluloses, proteins, pectins, lipids. . .) are used. Each class contains biopolymers that can be very different in terms of molar weight, polymerization degree as well as transport properties (diffusivity), solubility, etc.

Besides, thermo-mechano-chemical processes in TSE exhibit uses and possibilities advantages which become disadvantages for their modeling. If combination of thermal, mechanical and chemical effects in a same continuous reactor allows the development of a lot of different processes, it also leads to a high phenomena interdependence. The main difficulty lies in the coupling between the particle and intraparticle physicochemistry of the vegetal matter on one hand, and the mechanical and transport phenomena on the other hand. Their links are direct via operation like crushing or compression, as well as indirect via the residence time and consequently via the reaction or the adsorption process. Furthermore, an important retroaction of the screw element geometry on the behavior within the previous elements prevails. This complex interdependence is illustrated on the Fig. 2.

This complexity lead N'Diaye et al. (1996) [9] to use the chemometrics approach of experimental design and response surfaces study in order to optimize at first the process. The following step, as it has been developed by many authors for polymer and food [13–15], is to study the matter transport via the residence time distribution (RTD) method. This approach will allow to understand the different behavior of the two phases from a global point of view and to propose explanations of the behavior of the TSE as a thermo-mecano-chemical reactor. RTD will then be considered as global responses of the system, and thus account for all internal phenomena affecting the local properties such as rheological characteristics (see Fig. 2). RTD analysis is nevertheless impeded by the incomplete filling of the TSE under standard operating conditions and by the lack of precise knowledge of the TSE filling rate.

In this work, the RTD in the TSE are obtained using a colored tracer technique. The classical reaction engineering approach is adopted to compare the RTD results with various models. In addition to continuous process parameters (i.e. screw rotational speed, feed

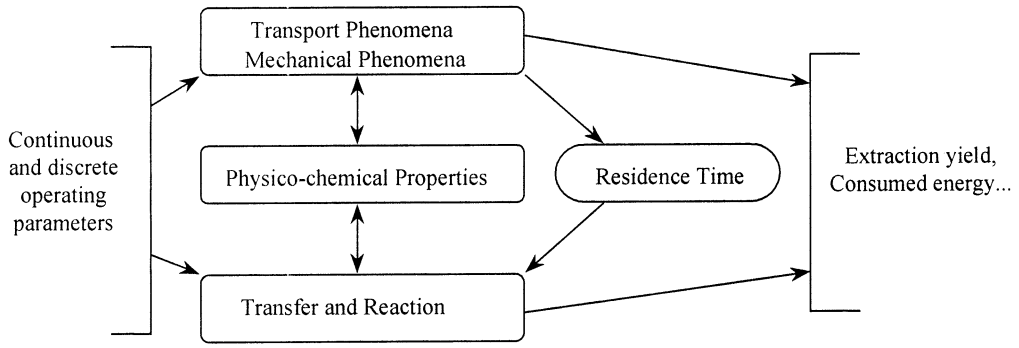

Fig. 2. Interdependence between phenomena in the TSE.

rates and NaOH concentration), the influence of discrete parameters are also studied (screw geometry). The following part of this paper presents the matter, the material, the experimental and the numerical methods used in this work. The next part is devoted to the results and their analysis.

3. Matter, material, experimental and numerical methods

3.1. Feedstock

Debarked chips of populus are ground to an average size of $15 \times 2 \times 2$ mm using an Electra type VS1 industrial grinder. The composition of the wood chips is determined using American Standard Test and Measurement methods (ASTM D-1103, D-1106, D-1787). The wood contains 52% of cellulose, 21–24% of lignin, 16–19% of hemicelluloses, some pectins, proteins, aromatic compounds and aliphatic acid. The moisture content of the initial chips is about 4%. Wood chips are fed in from a bin via a feeding screw and a chute (see Fig. 1 for reactor design).

The extractive solutions are injected using a volumetric pump at a single point located 180 mm from the beginning of the screw.

3.2. Twin screw extruder

Experiments are performed using a modified clextral BC45 TSE (see Fig. 1). It is a fully intermeshing corotating twin-screw extruder. Seven sections form the 1.4 m long barrel. Four sections are heated by induction belts and cooled by water circulation. Conical holes (inlet diameter: 1mm; outlet diameter: 2 mm; eight holes per cm^2) in a plate form the filter element added at the end of the barrel in order to extract the liquid from the output slurry. The die consists of a 25 mm long cylindrical hole, 12 mm in diameter. Five different kinds of elements are used in the axis profile: T2F (trapezoidal two-flight screw), C2F (two-flight screw), MAL2 (bi-lobe kneading element) always positioned with a $\pi/2$ shift (i.e. in a neutral position for transport compared with conveying screw elements), MAL0 (right-handed mono-lobe kneading element) and C2FC (reversed two-flight screw element). 100 mm length elements were principally used but 50 mm length elements were also available. The usual qualitative effects of these elements are reported on Table 1 [8–13]. The pitch of the transport screw elements varies from 66 to 25 mm. All experiments are carried out with a reverse screw element with peripheral slots grooved in the screw flight for leakage flow.

3.3. Experimental processing

The processing domain is limited by several conditions [8]. Clogging of the reactor has to be avoided, but more important is the correct functioning of the reversed screw elements. It allows in particular the matter

Table 1
Elements effects

Element	Mixing	Shearing	Transport
Transport screw	+	+	+++
Kneading (mono-lobe)	+	++++	+
Kneading (bi-lobe)	++++	+++	Neutral
RSE	+++	+++++	–

Table 2
Experimental domain

	Symbol	Central point	Minimum	Maximum
Speed screw (rpm)	N	175	110	250
Solid feed (kg h^{-1})	Q_S	4.8	3.2	6.7
Liquid feed (kg h^{-1})	Q_L	36.5	21.5	51.5
NaOH massic % in liquid	σ	5	3	7

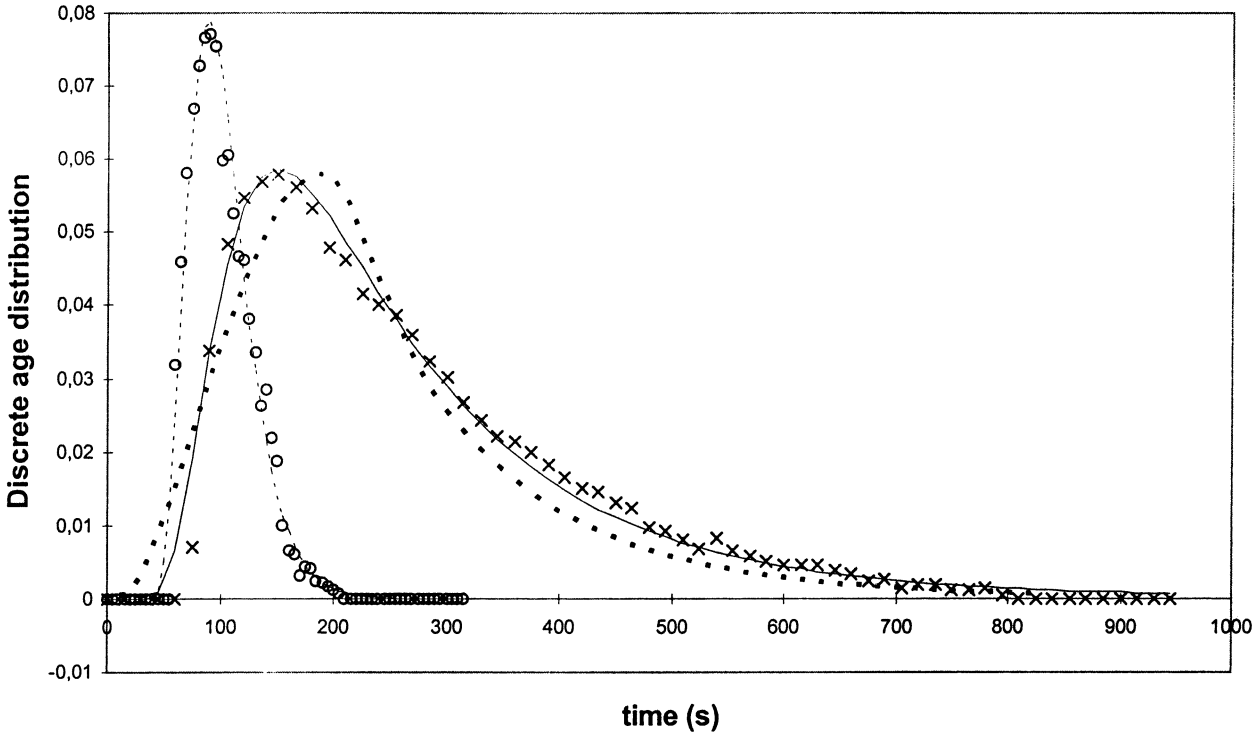

Fig. 3. Experimental RTD at central functioning point for liquid (o) and solid (×) phase. Model A RTD for liquid (- -) and solid (· · ·) phase, model B for solid phase (—).

to form a 'plug'. This plug is necessary to press the solid in order to separate the two phases, but unfortunately, it only appears under specific conditions. Furthermore, the RSE can totally stop the transport of solid matter and, as a consequence, the TSE too. Consequently, the authorized range of parameter variation is restricted around a central functioning point defined in terms of screw rotational speed N, solid feed rate Q_S, liquid feed rate Q_L and NaOH concentration σ. Variation ranges of these parameters are reported on Table 2. All the experiments are conducted at a fixed barrel temperature of 55°C, that is the upper limit temperature to avoid hemicelluloses chemical transformation. For the study of the profile influence, only the kneading elements and RSE are replaced in half or totality by 33 mm pitch transport elements.

For all experiments, the following parameters are measured:

- the liquid and solid reactor output rates needed to perform mass balances;
- I, the electrical intensity used by the engine. It is related to the torque applied on the screws via a linear relation and characterizes the mechanical energy transmitted to the matter;
- P, the pressure exerted by the matter on the screw profile in the longitudinal axis. It is measured on the decoupler;
- ω, the solid weight percentage in the exiting solid phase. It characterizes the solid/liquid separation and appears in the mass balance.

All these parameters shall be qualified as responses of the system.

Steady state conditions are followed by two different experimental investigations. First, the RTD of each phases in the TSE are determined using two erythrosin tracer techniques. Then, the extruder is suddenly stopped and opened in order to observe the inside matter location.

The erythrosin tracer was chosen by N'Diaye [8] for its neutral characteristics with respect to the process and to the good colorization of most of the vegetable matter, itself often highly colored. In the case of the liquid RTD determination, the tracer is directly incorporated in the liquid flow at the entrance of the reactor, thanks to a small derivation very close to the RSE and automatic valves. In the case of the solid RTD determination, some colored wood chips are directly put on the first screw element. The colored matter injection in both cases is small enough in mass (2 g for the liquid and 5 g for the solid) and time (<2 s), compared to the flow rates and to the mean residence times, to be considered as a Dirac pulse. Because of the reactor configuration, no experimental verification can be carry out, nor intermediary samples can be taken along the reactor. 5 ml samples of liquid every 3 s and 5 g samples of solid every 10 s are taken at the liquid and solid outlets of the apparatus. All samples are stored in a 4°C room until being analyzed.

Table 3
Experimental and RTD identification results

Continuous parameters				DTS identification results					System responses		
N (rpm)	Q_L (kg h^{-1})	Q_S (kg h^{-1})	σ (%)	τ_L (s)	Pe_L	τ_{S1} (s)	τ_{S2} (s)	Pe_S	I (A)	ω	P (Bar)
175	36.5	4.12	5	45.19	57.98	39.34	224	1.5	25	47	21
250	36.5	4.12	5	27.39	41.1	22.32	191.6	1.88	20	43	14
213	51.5	4.12	5	29.6	35.96	23.08	28.2	1.56	19	45	13
138	21.5	4.12	5	74.79	42.92	46.86	267.8	1.92	32	49	251
138	51.5	4.12	5	41.06	36.23	54.18	294.1	0.616	27	47	25
100	36.5	4.12	5	85.45	32.41	75.37	300.7	1.5	36	52	35
213	21.5	4.12	5	46.06	37.85	16.35	249	2.7	24	46	17
175	36.5	4.8	5	45.69	37.9	31.02	174.06	3	27	46	20
175	36.5	4.8	7	48.41	89.1	27.61	182.43	2.33	28	46	16
175	36.5	4.8	3	54.91	48.8	27.8	189.12	3.95	36	47	26
175	36.5	6.67	6	53.13	40.4	37.17	141.91	2.61	33	41	16
175	36.5	3.2	4	69.78	49.3	40	220	2	29	50	25
175	36.5	3.2	6	52.79	43.2	30.03	206.25	3.22	21	45	16
175	36.5	6.67	4	63.75	29.4	33.68	131.6	4.36	33	39	15

3.4. Experimental analysis method

Colored outlets samples are analyzed by colorimetry. Liquid phase absorption is measured but not directly on the sample because hemicelluloses present in the solution absorb at the same wave length (538 nm). Samples pH is decreased to 4 when 2 volumes of alcohol are added in order to precipitate the hemicelluloses. Then, solutions are filtered and the absorption is measured.

Each solid phase sample is ground to homogenize the color and to eliminate large size particles which disturb measurements. The absorption is then directly measured on the ground samples.

3.5. RTD models identification

The RTD data are examined through typical distribution versus time plots. RTD is defined as:

$$E_i = \frac{C_i}{\sum_{i=1}^{n} C_i \Delta t} \tag{1}$$

where C_i is the tracer concentration in each sample and Δt is the sampling period.

Typical curves are shown on Fig. 3 for the solid and liquid RTD, respectively. All the solid RTD have the same shape: a time delay of 40–50 s and then an increase to reach a maximum within 20–30 s, followed by a slow decrease until zero in 500–600 s. Liquid RTD are more symmetrical around a 40–50 s maximum. Many authors proposed models to represent transport in TSE by a combination of tubular reactors and a cascade of continuous stirred tank reactors (for the extrusion of rice starch [14], or for wheat starch [15,16]). In this work, two different models were used: model A, an axial dispersive tubular reactor model (a two parameter model: the mean residence time τ and the Peclet number Pe) and model B, where an axial dispersive tubular reactor is associated in series with a tubular reactor (a three parameter model: the mean residence time in the tubular reactor τ_1, the mean residence time in the dispersive tubular reactor τ_2, and the Peclet number Pe). For both dispersive tubular reactors, closed/closed boundary conditions are used. In the axial dispersive tubular reactor, Pe and τ are defined by the following equation obtained from a mass balance on the tracer:

$$-\frac{L^2}{\mathrm{Pe}} \cdot \frac{\partial^2 C(z,t)}{\partial z^2} + L \cdot \frac{\partial C(z,t)}{\partial z} + \tau \cdot \frac{\partial C(z,t)}{\partial t} = 0 \tag{2}$$

where $C(z,t)$ is the tracer concentration, (Oz) the longitudinal axis, t the time and L the reactor length. Because of the different positions of the two phases outlets, the considered length of the reactor is 1.2m for the liquid and 1.4m for the solid.

RTD are numerically treated in order to identify models parameters by using a Gauss–Newton based minimization method in the Laplace domain. Fast and Inverse Fast Fourier Transformation are used to translate RTD in the real time or in the Laplace's space. It has been verified that same results were obtained with minimization in the real time domain.

Both models were tested upon the solid and liquid RTD. Model A and B give the same fitting for the liquid phase, so model A will be used for this work (the parameters will then be noted τ_L and Pe_L). As shown on Fig. 3, model B gives the best fitting of the experimental data for the solid RTD, and it will then be used in this study (the parameters will be noted τ_{S1}, the mean residence time in the tubular reactor, τ_{S2}, the mean residence time in the dispersive tubular reactor and the

Peclet number Pe_S). It is to be noticed that these models fit experimental RTD quite well, with a few parameters, and, as a consequence, it wasn't necessary to increase the complexity of the representation with more detailed models.

All results related to the RTD chosen model parameters identification are reported on Table 3.

Influence of the continuous parameters on the RTD responses is expressed according to the interpolation Doehlert's method (1970) [17,18] in term of polynomial functions [19], for the mean residence times, the Pe, I, P and ω.

The experimental data are represented in the next paragraphs by these interpolation polynomial functions. In the case under consideration, experiments are so long and difficult to perform that this experimental method was the only one able to give sufficient data to choose a functioning point and to examine the influence of the parameters.

4. Results and discussion

4.1. Visual observation

Stopping and opening the reactor under steady-state conditions allow to observe qualitatively the location of the solid and the local filling rate of the reactor. Notice that the reactor opening induces a loss of the liquid phase and 10–20% of the solid phase. Only a qualitative analysis of the extruder process run is then possible. Most of the solid is in the RSE, in the half part of the transport element located just before the RSE and in the two kneading elements. Overall, the reactor can be separated into two parts: before the RSE, the two phases (liquid and impregnated solid) are present, whereas only impregnated solid can be found from the RSE to the die. In this second part, the under-pressured elements (i.e. the RSE and just before the die) are totally filled with solid matter. That is not the case in the first part of the reactor. As it has been mentioned previously, the TSE is not totally full of matter under usual working conditions. Such a visual observation point out that the variations of the filling rate are significant in the kneading elements, but the occupied volume is not accessible because of the compressibility of the matter.

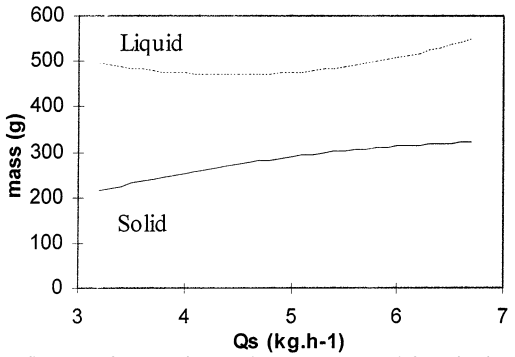

Fig. 5. Influence of Q_S on internal mass at central functioning point.

4.2. Global approach: continuous parameters influence

All RTD shapes being identical, the results are presented in terms of mean residence times and internal mass (product of the mean residence time by the feed rate) in the first part, and in terms of Pe and axial dispersion coefficients (D) in the second part. The last paragraph concerns some considerations about links between the axial pressure, the engine intensity and the solid weight percentage in the exiting solid phase.

4.2.1. Mean residence times and internal mass

Observed τ_L vary from 30 to 85 s (see Table 3). The τ_{S1} varies from 15 to 75 s. The τ_{S2} varies from 120 to 300 s. Total solid residence time ($\tau_{S1} + \tau_{S2}$) is then more important than the liquid one. This fact can be explained by the presence of the solid in the two parts of the reactor, especially in the second part where the filling rate is the more important, and, as a consequence, the residence time.

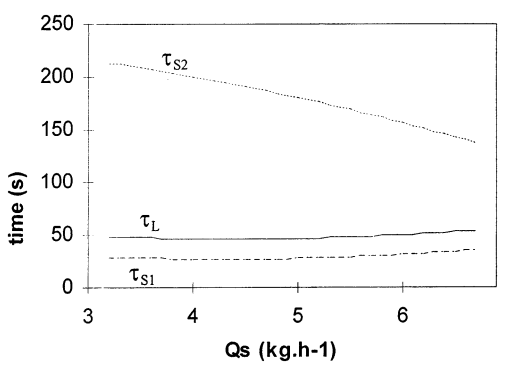

Fig. 4. Influence of Q_S on mean residence times at central functioning point.

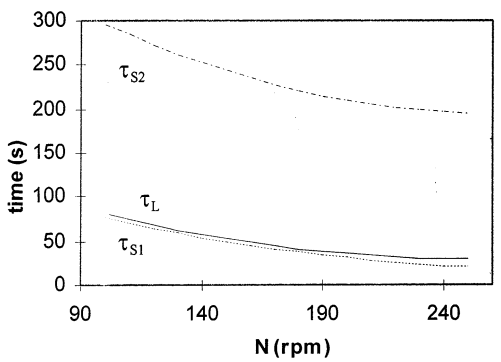

Fig. 6. Influence of N on mean residence times at central functioning point.

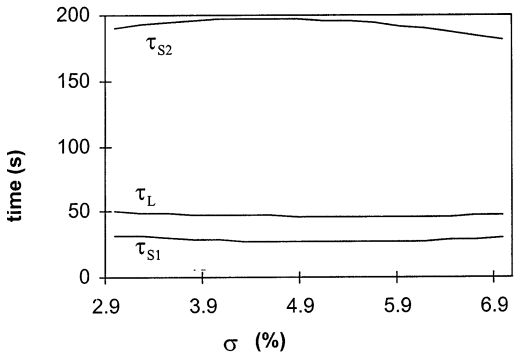

Fig. 7. Influence of σ on mean residence times at central functioning point.

4.2.1.1. Influence of Q_S. Fig. 4 and Fig. 5 show the evolution of τ and of the internal mass respectively with the solid feed state Q_S. An increase in Q_S value decreases the total solid mean residence time ($\tau_{S1} + \tau_{S2}$) (Fig. 4), but also contributes to fill the reactor with the solid phase (Fig. 5), in the kneading elements especially (see Section 3.1). The relative effect of Q_S is more important on τ_{S2} than on τ_{S1}, suggesting that τ_{S1}, and therefore the tubular reactor model, is linked with the first part of the reactor (until the RSE) whereas τ_{S2}, and then the dispersive tubular reactor model can be principally associated with the second part. As visual observations showed, the second part of the TSE is full of solid matter. As a consequence, an increase of Q_S can only act on τ and not on the filling rate in this second part. This is not the case in the first part of the TSE, where then, the effect of τ_{S1} is preponderant.

These links between τ_{S1} and the first part and between τ_{S2} and the second part of the reactor are a simplified way of considering the problem though. It will only help to analyze the parameters influences on the mean residence times.

In addition, no significant influence of Q_S on the transport parameters of the liquid phase could be inferred from the experiments.

4.2.1.2. Speed screw N influence. Fig. 6 shows the effect of N on τ_L, τ_{S1} and τ_{S2}. As it can be expected, they all decrease with N. In the conveying screw elements, this effect of N can be explained through the matter velocity. This velocity can be related to N.p in a first approximation (where p is the pitch of the screw) and consequently, as N increases, residence times of both solid and liquid phases decrease in the conveying screw elements. In the kneading elements, it is not possible to explain easily the influence of N upon the behavior of the matter and upon the residence times. Therefore, visual observations show that the quantity of matter and then the filling rate in these elements decrease with an increase of N. As there is no changes in the feed rates, the internal mass varies according to the residence times.

4.2.1.3. NaOH percentage σ influence. As displayed on Fig. 7, no influence of NaOH percentage σ on the liquid or solid residence times is inferred. NaOH is used for the reaction and the extraction of hemicelluloses, and the reactive fractionation (delignification) of the matter. The alkaline solution also acts as a lubricant of solid/solid contacts (vegetable matter/barrel and vegetable matter/screw). Without NaOH, solid can not pass through the RSE and the reactor is blocked. This action on the behavior of the matter is not directly linked with the RTD but with the difficulty for the solid matter to pass through the kneading elements and particularly through the RSE, and, as a consequence, the NaOH percentage has a great influence on the energetic consumption.

4.2.1.4. Liquid feed rate Q_L influence. The mean residence time for the liquid phase τ_L decreases and internal liquid mass (and then the filling rate) increases with the rising of Q_L, as shown in Fig. 8 and Fig. 9. Q_L does not act on the solid phase behavior, but determines the NaOH mass in the system and, consequently, its lubrication effects that helps the solid matter to pass through the kneading elements, so the energetic consumption of the TSE.

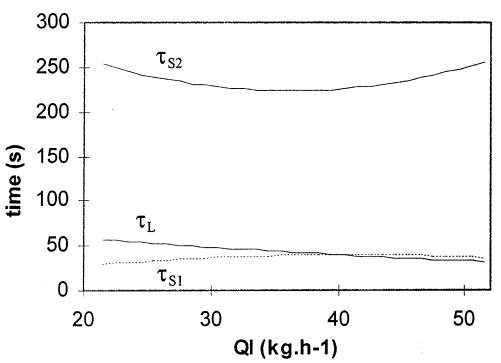

Fig. 8. Influence of Q_L on mean residence times at central functioning point.

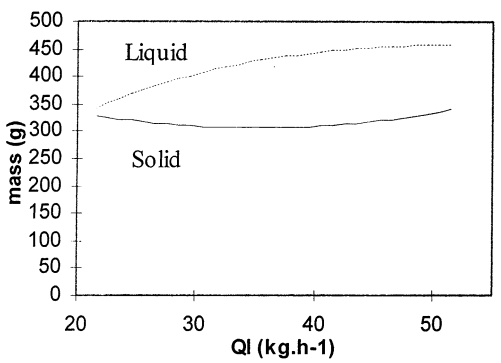

Fig. 9. Influence of Q_L on internal mass at central functioning point.

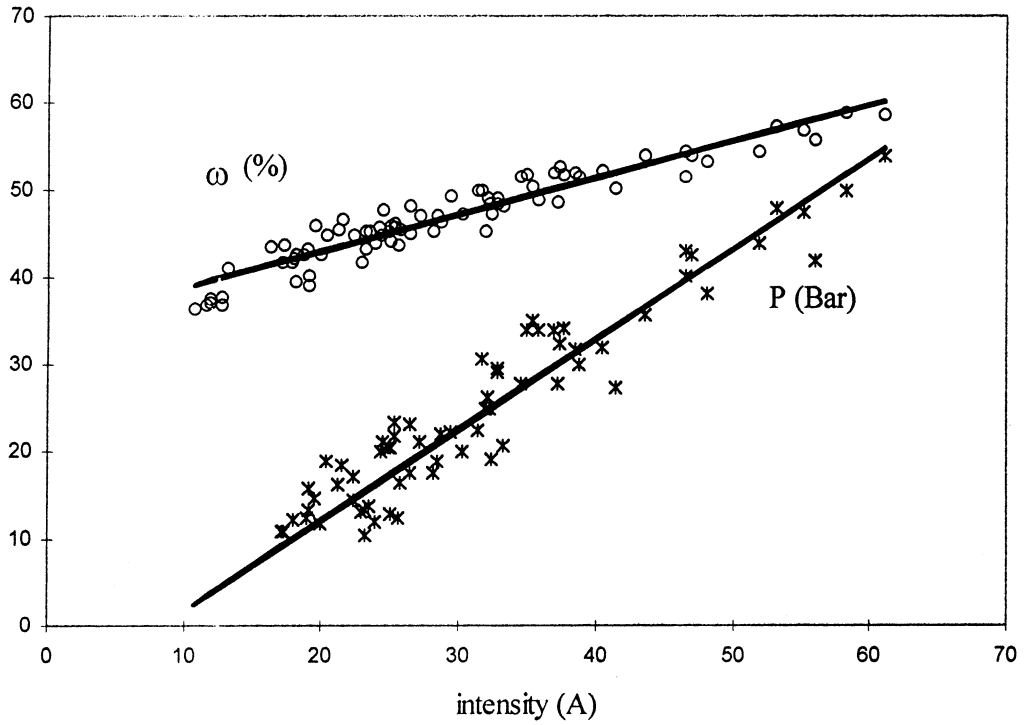

Fig. 10. ω and P function of I in all observed conditions.

4.2.2. Peclet numbers

Table 3 shows the identified Peclet numbers. As seen in Fig. 3, there is a large difference between solid and liquid RTD in terms of Pe. The Pe_L vary from 15 to 100 under the examined conditions. The dispersive effect for the liquid phase comes essentially from the kneading elements in the screw profile.

The Pe_S vary from 1 to 4. As seen before (see Section 3.1), the axial dispersive tubular reactor model for the solid RTD can be linked with the second part of the reactor. As a consequence, the major dispersive effects that are observed are located in the RSE and concern solely the solid phase. The reactor can be considered like an association in series of a tubular reactor and a continuous stirred vessel as far as the solid phase is concerned.

Because of the relative low sensibility of the Pe parameter during model identification, especially on Pe_L, even a qualitative analysis of Pe variations can not be performed.

4.2.3. Intensity, pressure and solid weight percentage in the exiting solid phase

The experimental intensity I varies from 10 to 60 A, P, from 15 to 60 bar and ω, from 35 to 60%.

In preliminary results, it is to be noticed that I, P and ω are related by means of quite linear relations (Fig. 10). As I characterizes the electrical energy consumed by the engine, these linear relations suggest that the mechanical energy transmitted to the matter is mostly used for the matter compression. This compression influences also transport phenomena as it increases the solid/solid (vegetable matter/barrel and vegetable matter/screw) friction and then influences the local speed of the matter in the TSE. This hypothesis seems to be confirmed by the relation between P and ω which characterizes the separation of the two phases, and then the pressure exerted in the RSE.

The variations of I, P and ω can be linked to the solid internal mass. Fig. 11 represents an I versus solid internal mass plot. The more the reactor is filled, the more the torque applied on the screws is important. This fact can be explained by the vegetable matter/barrel and vegetable matter/screw surfaces increase with the solid internal mass, and then by the increase of the friction.

4.3. Contributions of the screw elements to the global residence times

4.3.1. Objectives, assumptions and methods

For solid/liquid extraction, the contact time duration between the two phases is of great importance. The objectives of the second part of this work is to present a first approach in the determination of the contributions of the screw elements to the global residence times. All experiments were performed at the central functioning point for the continuous parameters (Section 3.3). The screw profile was modified in order to characterize the influence of the different screw ele-

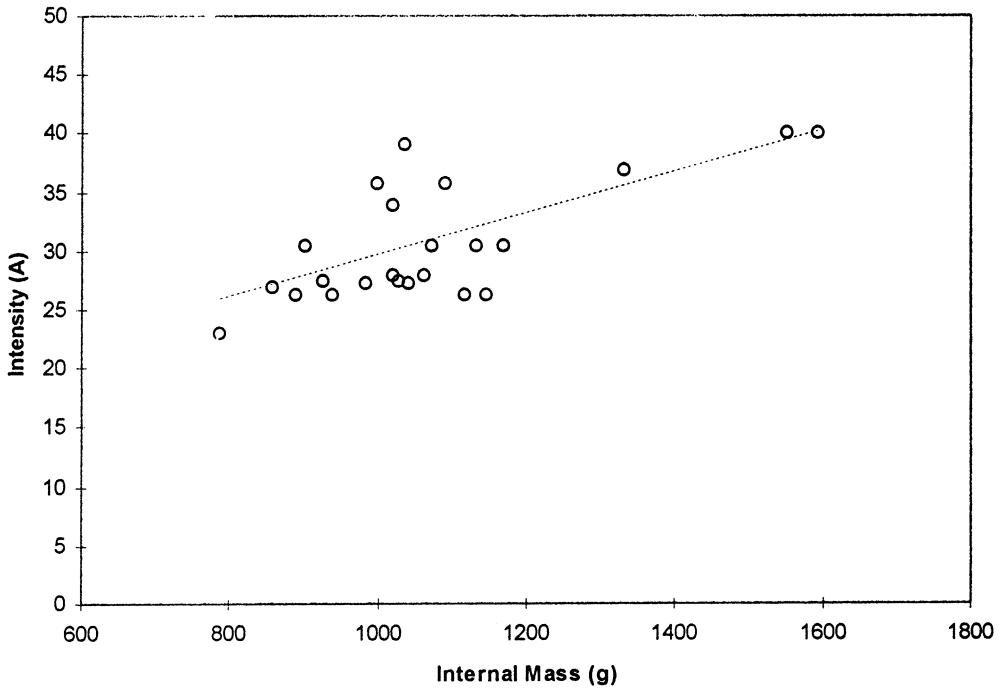

Fig. 11. Relationship between I and the solid internal mass in all observed conditions.

ments. The kneading elements and RSE are replaced in half or totality by 33 mm pitch transport elements. Table 4 shows the experimental conditions and the corresponding results of RTD models identification. These results are then valid only for the specified continuous parameters values. So they have to be considered in a qualitative point of view, allowing to give a more physical interpretation of the previous results, and to verify the links of the RTD models with the different parts of the TSE.

In this study, two drastic simplifying hypothesis are set: (i) mean residence time in standard screw element is proportional to the pitch, (ii) the elements position does not influence their behavior. It is then possible to consider the global mean residence time as the sum of each element contribution and to identify each element mean residence times by minimizing the discrepancy between model and experimental mean residence times. No assumptions are made on the contribution, or not, of the elements upon one or another model, or part of a model. Four contributions have to be identified:

- τ_{MAL0}, the mean residence time in a MAL0 element;
- τ_{MAL2}, the mean residence time in a MAL2 element;
- τ_{RSE}, the mean residence time in a RSE element;
- τ_{S33}, the mean residence time in a conveying screw with a 33 mm pitch.

The contribution of the other conveying screw element is deduced from τ_{S33} by multiplying τ_{S33} by the ratio of the pitches. The results of the identification are shown in Table 5, and Fig. 12 represents the identified mean residence times versus the experimental residence times, showing the quite good fitting of the identification.

4.3.2. Results

As expected, for solid or liquid phase, τ_{MAL0}, τ_{MAL2} and τ_{RSE} are much more important than τ_{S33}, the mean

Table 4
RTD identification results

Discrete parameters			DTS identification results				
MAL2 length (mm)	MAL0 length (mm)	RSE length (mm)	τ_L (s)	Pe_L	τ_{S1} (s)	τ_{S2} (s)	Pe_S
50	50	100	17.82	22.56	10.88	89.13	1.07
50	50	50	29.4	15.21	25.25	56.56	2.95
0	50	50	18.22	21.46	22.63	56.57	2.2
100	50	50	38.51	26.38	48.59	82.1	3.48
50	0	50	25.4	9.857	28.59	66.9	3.15
50	100	50	37.52	26	28.67	71.02	3.66
50	0	100	31.42	27.56	17.33	85.51	5.43

Table 5
Elements contributions to the mean residence times

Element	τ_L (s)	τ_{S1} (s)	τ_{S2} (s)
Screw 66 and screw 50	1.7	1.5	4.4
Screw 25	2.0	1.7	5.0
Screw 33	1.5	1.3	3.8
MAL2	13.1	12.9	21
MAL0	13.6	13.3	5.4
RSE	0	0	58

residence time in the conveying screw. There is no contribution of the RSE to τ_L, or to τ_{S1}.

RSE elements do not contribute to the liquid mean residence time τ_L because solid/liquid separation occurs at the very beginning of the RSE. Moreover, for the solid mean residence times, the RSE contribute only to τ_{S2}. As all dispersive effects are accounted by the tubular reactor with axial dispersion model, this fact confirms the important dispersive effect of this element. The matter is submitted there to opposite flows (towards the die through the slots because of the global flow and pressure, and towards the filter because of the geometry of the reversed elements).

The contributions of the two kneading elements hide different phenomena. In these elements, there is an accumulation of solid in 'matter plugs' which implies the increase of filling rate for the liquid phase upstream these elements. The model and identification method do not allow to distinguish these effects.

The quite similar values of the contributions for τ_L and τ_{S1} suggest co-current flows for the two phases in the first part of the reactor before the RSE. Since the values of the contributions of τ_{MAL0} and τ_{MAL2} to τ_{S2} are not equal to 0, it points out the limit in the idea that each part of the models can be linked directly to a physical area in the TSE.

Even though the hypothesis are very simple, the results obtained with this contributions method confirm the usual qualitative results (see Table 1) concerning with conveying, kneading or reversed screw elements effects. It allows to use general considerations to choose the screw profile for vegetable matter extrusion and to have approximated local residence time values. Besides, it is very encouraging, as shown in Fig. 12, that this contribution method leads to satisfactory results, concerning the global residence times when changing (of course not drastically) the profile of the screw.

5. Conclusion

Problems generated by the complexity of the vegetable matter and by the important coupling of the phenomena in a closed reactor are numerous. However, this work shows that it is possible to ameliorate the knowledge on this kind of reactor using chemical engineering usual methods.

Through visual observation and chemical engineering analysis, this work shows that the reactor consists in two parts: one where the two phases (liquid and solid) flow co-currently, and one containing impregnated

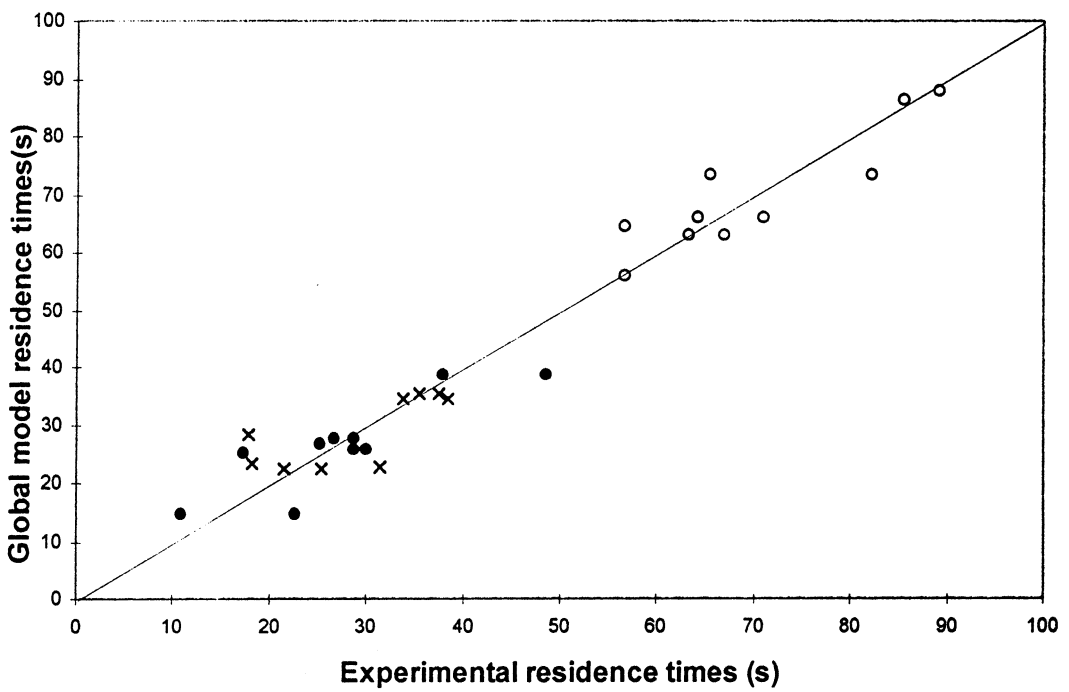

Fig. 12. Modeling versus experimental residence times for τ_L (●), τ_{S1} (X) and τ_{S2} (○).

solid only. As far as solvent extraction is concerned, the first part is the more important because it is where the extractive reaction occurs. The second part, from the RSE to the die, is necessary for the solid/liquid separation and as a consequence for the correct functioning of the reactor.

RTD study allows to point out the continuous parameters influence. This influence concerns the mean residence time and the internal mass of matter (or the filling rate of the reactor if the matter is considered incompressible in a first approximation). But, because of the high difference of the mean residence time value between the first and the second part of the reactor, an accurate analysis of the parameters influences upon the first reactor part residence time is difficult. Local RTD will have to be performed in order to obtain more precise information, but in practical, it is not yet possible. However, even if no predictions can be made through such an approach, it is possible to estimate the role played by each of the screw elements and to distinguish their actions on both liquid and solid phases. This understanding will be necessary to imagine a more physical representation, allowing the prediction of the global behavior of these new type of extractor.

Appendix A. Nomenclature

C_i	tracer concentration (g m^{-3})
D	axial coefficient of diffusion (m^2 s^{-1})
E_i	discrete residence time distribution function (s^{-1})
I	engine consumed intensity (A)
L	reactor length (m)
N	screw rotational speed (rpm)
P	axial pressure (bar)
Pe	Peclet number
Q_S	solid feed rate (kg h^{-1})
Q_L	liquid feed rate (kg h^{-1})
Greek letters	
σ	NaOH massic percentage in liquid phase
τ_L	liquid phase mean residence time (s)
τ_{MAL0}	MAL0 residence time contribution (s)
τ_{MAL2}	MAL2 residence time contribution (s)
τ_{RSE}	RSE residence time contribution (s)
τ_{S1}	solid phase mean residence time for tubular reactor part (s)
τ_{S2}	solid phase mean residence time for axial dispersive tubular reactor part (s)
τ_{Sp}	conveying screw with a pitch of p residence time contribution (s)
ω	Solid weight percentage in the exiting solid phase

References

[1] J.M. Harper. Food extruders and their applications, In: C. Mercier, P. Linko, J.M. Harper (Eds.), Extrusion Cooking, AACC, St Paul MN, 1989, pp. 1–16

[2] P. Colonna, A. Buleon. Transformations structurales de l'Amidon, In: P. Colonna, G. Della Valle (Eds.), la Cuisson-extrusion, Lavoisier Tec. et Doc., Paris, 1994, pp. 2–13.

[3] N. Bouzid, G. Vilarem, A. Gaset, Extraction des huiles essentielles par des techniques non conventionnelles, Revista Italiana E.P.P.O.S., Agosto '97, 1997, pp. 3–11.

[4] S. Isobe, F. Zuber, K. Uemura, A. Nogushi, A new twin-screw press design for oil extraction of dehulled sunflower seeds, J. Am. Oil Chem. Soc. 69 (9) (1992) 884–889.

[5] G. Anon, Procédé et installation de traitement en continu d'une matière cellulosique, French patent: 78 05 495, 1978.

[6] C. De Choudens, R. Angelier, Les pâtes chimicothermomécaniques blanchies obtenues avec le procédé bi-vis, Revue ATIP 3 (44) (1990) 137–146.

[7] L. Rigal, Technologie d'extrusion bi-vis et fractionnement de la matière végétale, 40 ans d'extrusion bi-vis chez CLEXTRAL, Recueil de conférences, Firminy (France), 8–10 October, 1996.

[8] S. N'Diaye Fractionnement de la matière végétale: mise au point d'un procédé thermo-mécano-chimique et modélisation du réacteur bi-vis. doctorat thesis INPT, Toulouse, France, 1996.

[9] S. N'Diaye, L. Rigal, P. Laroque, P.F. Vidal, Extraction of hemicelluloses from poplar, populus tremuloides, using an extruder-type twin screw reactor: influence of the main factors, Biores. Techol. 57 (1996) 61–67.

[10] P. Colonna, J. Tayeb, C. Mercier, B. Vergnes, Flow mixing and residence time distribution of maize starch within a twin-screw extruder with a longitudinally-split barrel, J. Cereal Sci. 1 (1983) 115–125.

[11] W. Szydlowski, R. Brzoskowski, J.L. White, Modelling flow in an intermeshing co-rotating twin-screw extruder: flow in kneading discs, Int. Polymer Process. 4 (1998) 207–214.

[12] J. Tayeb, B. Vergnes, G. Della Valle, A basic model for a twin-screw extruder, J. Food Sci. 54 (1989) 1047–1056.

[13] L.P.B.M. Janssen, Twin-screw extrusion, Elsevier, Amsterdam, 1978.

[14] R.E. Altamore, P. Ghossi, An analysis of residence time distribution pattern in a twin-screw cooking extruder, Biotechnol. Prog. 2 (3) (1986) 157–163.

[15] P. Boissonat, Etude paramètrique et modélisation des écoulements de la matière par analyse de la distribution des temps de séjour dans trois cuiseurs extrudeurs bi-vis, doctorat thesis, Université de Technologie de Compiègne, 1990.

[16] A. Yeh, S. Hwang, J. Guo, Effects of screw speed and feed rate on residence time distribution and axial mixing of wheat flour in a twin-screw extruder, J. Food Eng. 17 (1992) 1–13.

[17] D.H. Doehlert, Uniform shell designs, J. R. Statist. Soc. 19 (1970) 231–239.

[18] A.I. Khuri, J.A. Cornell. Response Surfaces Designs and Analyses, Marcel Dekker, New York, 1987, pp. 105–148.

[19] Mathieu, D.R. Phan-Tan-Luu, New efficient methodology for research using optimal design (NEMROD software), LPRAI Center, Centre St Jerome, University of Aix-Marseille, France, 1992.